J. Biochem. 119, 1131-1142 (1996)

Sequential ^{1}H and ^{15}N NMR Resonance Assignment and Secondary Structure of Ferrocytochrome c_2 from *Rhodobacter sphaeroides*[1]

Pierre Gans,[*,2] **Jean-Pierre Simorre,**[*] **Michael Caffrey,**[*] **Dominique Marion,**[*]
Pierre Richaud,[†] **and André Verméglio**[†]

[*] *Institut de Biologie Structurale CEA-CNRS "Jean-Pierre Ebel," 41 Avenue des Martyrs, 38027 Grenoble CEDEX, France; and* [†] *Laboratoire de Bioénergétique Cellulaire, Département d'Ecophysiologie Végétale et Microbiologie, C.E.N. de Cadarache, 13108 Saint-Paul-lez-Durance CEDEX, France*

Received for publication, January 25, 1996

Sequence-specific ^{1}H and ^{15}N assignments have been made for the amino acids of the ferrocytochrome c_2 from *Rhodobacter sphaeroides*. Initial assignments were made by analysis of a series of homonuclear 2D COSY, TOCSY, and NOESY spectra obtained with the unlabeled protein. 2D and 3D ^{1}H-^{15}N correlated spectra obtained for a uniformly ^{15}N-labeled ferrocytochrome c_2 were used to confirm and extend the assignments. Partial ^{13}C assignments have also been made by means of HSQC experiments on ^{13}C at natural abundance, in particular for about two-thirds of the $^{13}C^\alpha$. Medium-range NOE connectivities, together with $^3J(HC^\alpha NH)$ coupling constants, indicated the presence of five helices at positions 6-16, 60-68, 74-82, 84-91, and 109-120. No other regular secondary structure was observed. This folding is similar to that previously observed for the ferrocytochrome c_2 of *Rhodobacter capsulatus* in solution, which exhibits approximately 50% sequence identity. Moreover, the rotation rates of the aromatic rings of phenylalanine or tyrosine, when conserved, were similar to those observed for *R. capsulatus*. Furthermore, $C^\alpha H$ chemical shifts, which are sensitive to the secondary structure and ring current effects of the heme, appear to be very similar for the two proteins. Consequently, the solution structure of *R. sphaeroides* ferrocytochrome c_2 appears to be very similar to that of *R. capsulatus* ferrocytochrome c_2. These results are compared with the X-ray crystal structure of the *R. sphaeroides* ferrocytochrome c_2.

Key words: cytochrome c_2, electron transfer, heme protein, multidimensional NMR, *Rhodobacter sphaeroides*.

In *Rhodobacter sphaeroides*, cytochrome c_2 is an electron carrier common to all the energetic pathways of the cell. It acts in the photosynthetic pathway as an electron donor for the reaction center and an electron acceptor for cytochrome bc_1, and takes part in the cyclic electron pathway across the membrane which generates the transmembrane field (*1*). It also participates in the aerobic respiratory pathway, transferring electrons from cytochrome bc_1 to cytochrome oxidase (*2*). Moreover, under denitrifying conditions, cytochrome c_2 carries out electron transfer between cytochrome bc_1 and the last three steps of this pathway: *i.e.* those involving nitrite reductase, NO-reductase, and N_2O-reductase (*3*). The key role of cytochrome c_2 in all these processes has been indicated by the inhibition of the last two respiratory processes by light, *i.e.* inhibition due in part to oxidation of cytochrome c_2 by the reaction center (*4-6*).

The interaction of the *R. sphaeroides* cytochrome c_2 with its partners in the photosynthetic chain (*i.e.* the reaction center and cytochrome bc_1 complex) has been extensively studied (for a review, see Ref. 7) since the three-dimensional structure of the *R. sphaeroides* reaction center is available (*8, 9*), as the light-induced redox change in the reaction center allowed precise measurements of all electron transfer reactions in the cytochrome c_2-reaction center complex. Despite numerous kinetic studies on the electron transfer *in vivo*, the mode of interaction between the reaction center and cytochrome c_2 is not well understood. The existence of two sites of interaction, distal and proximal, giving rise to slow and fast electron transfer steps, respectively, has been postulated from the results of *in vitro* studies (*10, 11*). However, this model has recently been questioned (*12, 13*). Morever, thermodynamic analysis of the electron transfer in whole cells of *R. sphaeroides* strain R26 led Joliot *et al.* (*14*) to postulate a supramolecular organization for the photosynthetic chain. The

---

[1] This work was supported in part by the Commissariat à l'Energie Atomique (CEA) and the Centre National de la Recherche Scientifique (CNRS). M. Caffrey gratefully acknowledges the generous support of the CEA. This is contribution n°303 of the *Institut de Biologie Structurale Jean-Pierre Ebel*, Commissariat à l'Energie Atomique/Centre National de la Recherche Scientifique.

[2] To whom correspondence should be addressed. Phone: +33 76 88 57 98, Fax: +33 76 88 54 94, E-mail: pierre@rmn.ibs.fr

Abbreviations: DQF-COSY, double quantum-filtered correlated spectroscopy; TOCSY, total correlated spectroscopy; NOE, nuclear Overhauser enhancement; NOESY, NOE correlated spectroscopy; HSQC, heteronuclear single quantum correlated spectroscopy; TPPI, time-proportional phase increment; WATERGATE, water suppression by gradient-tailored excitation; RC, reaction center; cytochrome bc_1, cytochrome bc_1 complex.

Downloaded from http://jb.oxfordjournals.org/ at Changhua Christian Hospital on October 2, 2012

supramolecular organization (or supercomplex) includes two reaction centers, one cytochrome bc_1 complex and one cytochrome c_2. In this model, the fast and slow phases of the cytochrome *c* photooxidation *in vivo* are related to the subsequent oxidation of cytochrome c_2 and cytochrome c_1, respectively. This supramolecular edifice is localised in the invaginated part of the membrane. A second pool, located in the periplasmic space, is implicated in the transfer between the cytochrome bc_1 complex and either cytochrome oxidase (*15*) or the enzymes of the denitrifying pathway (*16*).

Different models of electron transfer complexes between the reaction center and cytochrome c_2 have been proposed to calculate the electron transfer rate. They are essentially of two types: the first one is based on stabilization of the complex by complementation of charges between ionized residues at the surfaces of the two proteins (*8, 17, 18*). The second involves a more complex approach in which stabilization of the complex is linked to complementarity of the electrostatic fields at the surfaces of the proteins (*19*). The results, however, of these studies are not in agreement. The angle and the edge to edge distance between the cytochrome c_2 heme and the reaction center bacteriochlorophyll pair vary from one model to another (*c.f.* Ref. *19* for a discussion). A prerequisite for these two methods is, however, knowledge of the three-dimensional structures of the two partners of the complex, and no structure was available for the *R. sphaeroides* cytochrome c_2 until recently (*20*). Consequently, analysis of its electron transfer reactions (*e.g.* Ref. *19*) has involved models based on the X-ray structure of the cytochrome c_2 of *R. capsulatus* (*21*) or the cytochrome c_{550} of *Paracoccus denitrificans* (*22*). Nevertheless, the surface lysines of cytochrome c_2 have been demonstrated to play key roles in the interaction between the reaction center and cytochrome c_2 by chemical modification (*23*) and site-directed mutagenesis (*18*). It must be noted that these lysines have also been implicated in the electron transfer between cytochrome c_2 and complex bc_1 (*24, 25*). In general, no significant differences are observed for the backbone and buried side-chains of a protein between the structures determined by X-ray crystallography and NMR; in contrast, the positions of the solvent-exposed side-chains appear to be more variable (*26*). Determination of the *R. sphaeroides* cytochrome c_2 structure in solution is needed for full comprehension of the interaction between the different partners of the electron transfer reaction, and in particular between those of the supercomplexes.

We have therefore investigated the solution structure of *R. sphaeroides* ferrocytochrome c_2 by NMR spectroscopy. The first stage in any structure determination is the complete assignment of the proton resonances. In this paper, we report the quasi complete assignment of the ^{1}H and ^{15}N resonances by means of homonuclear and heteronuclear multidimensional NMR experiments. We have also determined the secondary structure of the polypeptide chain and have obtained some insight into the global fold of the cytochrome. Comparison with the X-ray structures of the cytochromes c_2 of *R. sphaeroides* and *R. capsulatus* is also discussed.

MATERIALS AND METHODS

Preparation and Labeling of R. sphaeroides Cytochrome c_2—*R. sphaeroides* cells were cultivated on degassed Hutner medium containing 1 μg/ml tetracycline under constant illumination. Unlabeled cytochrome c_2 was purified from different *R. sphaeroides* strains: the 2.4.1 strain, the R26 strain (the 2.4.1 strain devoid of carotenoid), and these two strains harboring the pC2.P404.1 plasmid containing the cytochrome c_2 gene (*27, 28*). The pC2.P404.1 plasmid and the 2.4.1 strain containing the plasmid were generously provided by Dr. Timothy Donohue. The R26 strain containing the pC2.P404.1 plasmid was obtained by conjugation of the R26 strain and the *Escherichia coli* S17-1 strain. It was determined that cytochrome c_2 production by the R26/pC2.P404.1 strain is 3 times that by the wild-type strain.

Large-scale cultures (30 liters) were performed by Equation Verte SARL (La Tour d'Aigues, France). The *R. sphaeroides* cytochrome c_2 was purified following the published procedure (*29*) with minor modifications. The uniformly ^{15}N-enriched (>98%) protein was obtained by growing *R. sphaeroides* strain 2.4.1/pC2.P404.1, a cytochrome c_2 overproducing strain, on a minimal medium containing 1 g/liter $^{15}NH_4Cl$ (Isotech) as the sole source of nitrogen. For the NMR experiments, electrophoretically pure samples of cytochrome c_2 were concentrated in the range of 2-6 mM in 0.1 M potassium phosphate buffer at pH 6.7 (uncorrected pH at 25°C) in 90% ^1H_2O/10% ^2H_2O or 100% ^2H_2O. The protein solution was deoxygenated with argon and the samples were kept reduced by the addition of a twofold molar excess of sodium dithionite in phosphate buffer under argon.

NMR—NMR experiments were carried with Bruker AMX spectrometers operating at proton frequencies of 400 and 600 MHz. The AMX 600 was equipped with a 5 mm Bruker probe with an internal pulsed B_0 field gradient coil. Two sets of homonuclear 2D correlation experiments were performed at 45 and 40°C. ^{1}H 2D DQF-COSY (*30*), TOCSY (*31, 32*), and NOESY (*33, 34*) spectra were recorded in the phase sensitive mode using the hypercomplex method (*35*). Water resonance was attenuated by means of coherent low-power presaturation ($\gamma B_2/2\pi = 50$ Hz) during the relaxation delay (1.2 s). For TOCSY and NOESY experiments, this presaturation was further combined with a "jump and return" read pulse (*36*). The WALTZ-17 mixing scheme used in TOCSY experiments was optimized to balance longitudinal and rotating frame cross-relaxation according to the technique known as clean TOCSY (*37*). TOCSY spectra were recorded with a isotropic mixing time of 80 ms including the delays of the clean TOCSY pulse scheme. The NOESY spectra were recorded with mixing times of 75 and 150 ms. In addition, to reduce the first-order phase correction in NOESY and TOCSY experiments, the first $90°_x$ pulse was replaced by a $360°_x$-$270°_{-x}$ composite pulse (*38*). Two-dimensional spectra were collected as 512 (t_1) and 1,024 (t_2) complex points with 32 scans per t_1 increment. Chemical shifts were referenced relative to the water resonance, calibrated in turn at 4.582 ppm at 45°C, and 4.629 ppm at 40°C with 2,2-dimethyl-2-silapentane-5-sulfonate. In order to solve various overlap problems, additional NOESY or TOCSY experiments were performed at 30 and 35°C.

2D Heteronuclear Spectroscopy—The pulse scheme used for the ^{15}N and ^{13}C HSQC experiments was similar to that of Bodenhausen and Ruben (*39*). Water suppression and

Downloaded from http://jb.oxfordjournals.org/ at Changhua Christian Hospital on October 2, 2012

coherence pathway selection were achieved with the AMX 600 by applying pulsed-field gradients as z-filters (*40*), and with the AMX 400 by the use of spin-lock pulses (*41, 42*). ^{1}H-^{15}N HSQC spectra were collected as 512 (t_2, ^{1}H) and 128 (t_1, ^{15}N) complex points with 4 scans per t_1 increment for the ^{15}N-labeled protein. ^{1}H-^{13}C HSQC spectra were collected as 1,024 (t_2, ^{1}H) and 256 (t_1, ^{13}C) with 64 scans per t_1 increment for the unlabeled protein. The spectral widths were: 3,623 Hz in F_2 (^{1}H=600.13 MHz) and 1,824 Hz in F_1 (^{15}N=60.8 MHz); 7,246 Hz in F_2 (^{1}H=600.13 MHz) and 12,072 Hz in F_1 (^{13}C=150.91 MHz). The carrier positions were 8.24 and 121.8 ppm for ^{1}H and ^{15}N, respectively; and 4.582 and 37.00 ppm for ^{1}H and ^{13}C, respectively. Quadrature detection in F_2 was achieved using the States-TPPI method (*43*). The WATERGATE sequence (*44*) was added for solvent suppression in the ^{15}N-HSQC experiments in order to avoid saturation of exchangeable amide protons during the relaxation delay. The 2D TOCSY-HSQC experiment on ^{13}C at natural abundance was similar to that of Medvedeva *et al.* (*45*). The spectral widths were 4,201 Hz in F_2 (^{1}H=600.13 MHz) and 12,072 Hz in F_1 (^{13}C=150.91 MHz). The carrier positions for ^{1}H and ^{13}C were 4.582 and 37.00 ppm, respectively. These spectra were collected as 512 (t_2, ^{1}H) and 150 (t_1, ^{13}C) complex points with 144 scans per t_1 increment.

Three-Dimensional Heteronuclear NMR—All 3D experiments were performed at 40°C. The 3D HNHA pulse scheme described by Vuister and Bax (*46*) was used. The spectral widths for ^{15}N, ^{1}H, and ^{1}H were 36, 5.50, and 7.22 ppm, respectively. The carrier positions for ^{15}N, ^{1}H, and ^{1}H were 121.8, 8.00, and 4.629 ppm, respectively. Spectra were acquired with a Bruker AMX 400, with 24 complex points in t_1, 50 complex points in t_2, and 48 scans per t_1/t_2 increment, resulting in a total experimental time of approximately 60 h. The 3D NOESY-HSQC and TOCSY-HSQC experiments were similar to the NOESY-HMQC (*47*) and TOCSY-HMQC (*48*) ones previously described. In addition, the WATERGATE sequence (*44*) was introduced for solvent suppression in the NOESY-HSQC experiments. For the TOCSY-HSQC experiments, the spectral widths for ^{1}H, ^{15}N, and ^{1}H were 6.409, 30, and 11.90 ppm, respectively. The carrier positions for ^{1}H, ^{15}N, and ^{1}H were 8.28, 121.8, and 4.629 ppm, respectively. Spectra were acquired with 128 complex points in t_1, 40 complex points in t_2, and 8 scans per t_1/t_2 increment, resulting in a total experimental time of approximately 60 h. For the NOESY-HSQC experiments, the spectral widths for ^{1}H, ^{15}N, and ^{1}H were 7.00, 30, and 11.902 ppm, respectively. The carrier positions for ^{1}H, ^{16}N, and ^{1}H were 9.11, 121.8, and 4.629 ppm, respectively. Spectra were acquired with 128 complex points in t_1, 40 complex points in t_2, and 8 scans per t_1/t_2 increment, resulting in a total experimental time of approximately 60 h.

The data were processed using either Bruker UXNMR software or the FELIX program (version 2.3; Biosym Technologies, San Diego, USA). For 2D data sets, in particular for the NOESY experiment, direct and indirect dimensions were multiplied by a squared sine bell function. They were transformed after zero-filling in the F_1 dimension, into 1,024 and 1,024 real points in F_1 and F_2 dimension frequency-domain spectra. The indirect dimensions of the 3D HNHA, NOESY-HSQC, and TOCSY-HSQC spectra were multiplied by a skewed sine-bell function and zero-filled. The final 3D matrices were 512×128×256 real points for the NOESY-HSQC and TOCSY-HSQC experiments, and 256×128×64 real points for the HNHA experiment. For convenient analysis of 3D data sets, 2D strip representations were generated as previously described (*49*).

Mass Spectrometry—Mass spectrometry analysis was carried out with a Perkin-Elmer Sciex API III-triple quadrupole mass spectrometer equipped with an electrospray source. The proteins were dissolved in a mixture of 20% methanol, 1% acetic acid, and water. The other conditions were as described by Petillot *et al.* (*50*).

RESULTS

Mass Spectrometry—Mass spectrometry experiments showed a molecular peak at 14,069 Da (±2.1 Da). This observation is in agreement with the theoretical mass of 14,068 Da expected from the amino acid sequence of the *R. sphaeroides* cytochrome c_2, with the presence of a pyroglutamate residue at the N-terminus (*51*). The mass spectrometry experiment also indicated the presence of another minor form of the cytochrome at M+17, depending on the type of cells used for purification of the sample (wild-type or overproducing strain).

NMR Results—In contrast to the reported spectra of other large class I cytochromes *c* [*e.g. R. capsulatus* cytochrome c_2 (*52*) and horse cytochrome *c* (*53*)], poor magnetisation transfer was observed in TOCSY spectra at temperatures below 40°C, even with mixing times greater than 100 ms. Neither variation of pH in the range of 5 to 7, nor modification of the ionic strength significantly improved the quality of the data. In our case, we found the optimal conditions to be temperatures of 40 and 45°C, pH= 6.8 and 100 mM phosphate buffer.

Spin System Assignments—Due to the high helical content of cytochromes *c*, most of the NH-C^{α}H correlations in the DQF-COSY experiment fell in the ranges of 7-8.5 and 3.5-4.5 ppm, leading to a very crowded spectrum in which only 80 individual cross-peaks could be observed. Nevertheless, using various temperature, we have been able to identify about 90% of the expected correlations. Although the usual pattern of Gly residues in COSY is strongly affected by line broadening, 14 (out of 15) glycines can be easily identified using the COSY and TOCSY spectra. The COSY experiments also allowed the identification of some NH-C^{α}H correlations exhibiting unusual chemical shifts (*e.g.* NH of G58, C^{α}H of E73, A9, V80, and D23). In addition, we observed, in the COSY experiment, the $C^{\delta}H_2$–N^{ϵ}H correlation for one arginine residue (R123). A representative TOCSY spectrum of the cytochrome c_2 of *R. sphaeroides* at 45°C is shown in Fig. 1. Through the TOCSY experiments, we have been able to observe correlations between the amide proton and side-chain for all the amino acids except the N-terminal residue (a pyroglutamate), the proline residues, and four other residues for which the amide proton resonances could not be observed (N33, K55, G56, and E107). For four other residues (V43, T50, Q51, and E73), only the correlations between the amide proton and C^{α}H were observable. Of the methyl-containing residues, we have been able to identify the eight valines, four of the five leucines, two of the three isoleucines, and five of the nine threonines from their characteristic pattern in the

Downloaded from http://jb.oxfordjournals.org/ at Changhua Christian Hospital on October 2, 2012

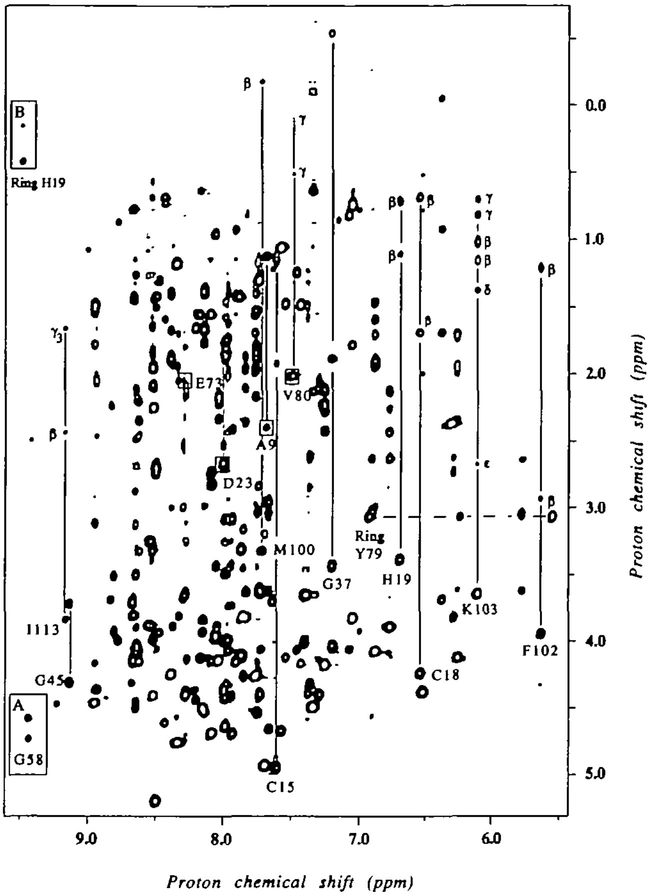

Fig. 1. **Amide/aromatic (F2)-aliphatic (F1) section of a TOCSY spectrum of *R. sphaeroides* ferrocytochrome c_2 acquired with an isotropic mixing time of 80 ms, in H_2O at 45°C and pH 6.7.** Complete spin systems are described for some residues including the heme ligands. The highly shifted H^α protons of A9, E73, and V80 are indicated. The connectivities between the ring protons of Y79 are shown. In the inserts are indicated the connectivities between the amide proton and the H^α protons of G58 (insert A), and between the N(1)H proton, and C(2)H and C(5)H of H19 (insert B). The chemical shifts of the N(1)H proton of H19 and the amide proton of G58 are 10.15 and 10.84 ppm, respectively. Correlations connecting the amide proton to the H^α, H^β, H^γ, H^δ, and H^ϵ protons are indicated by α, β, γ, δ, and ϵ, respectively.

TOCSY spectra. Two threonines (T50 and T91) depart from the usual pattern for this residue in the TOCSY spectra, as an additional signal, which disappears in D_2O, arises from the slow exchanging hydroxyl group. One arginine (R123) has been easily assigned from the repetition of the whole spin-system in the TOCSY spectrum. Serine 25 has also been identified from the characteristic chemical shifts of the $\beta\beta'$ protons. Methionine 100 was recognised from its unusual chemical shifts due the shielding effect of the heme ring. All other spin systems were identified during the sequential assignment process. Most of the spin system identifications were confirmed using a ^{15}N labeled sample and 2D HSQC (Fig. 2) or 3D HSQC-TOCSY experiments. A summary of the ^1H and ^{15}N assignments is given in Table I.

Sequential Assignments—The sequential assignment of the spin systems has been made using the NH_i-NH_{i+1}, $C^\alpha H_i$-NH_{i+1}, and $C^\beta H_i$-NH_{i+1} NOE connectivities. Despite the relatively large number of residues present, which leads to overlapping of correlations, the sequential assignment process was straightforward. Spin systems that could be unambiguously identified in the TOCSY and COSY experiments, and S25, which was the only serine in the sequence, were used as starting points for the assignment. Proline residues P5, P83, and P124 were positioned using the $C^\alpha H_{i-1}$-$C^\delta H_i$ cross-peaks with the preceding residue. Using medium range connectivities (*i.e.* $C^\alpha H$-NH_{i+2} and $C^\alpha H$-NH_{i+3}), we have been able to resolve an ambiguity arising from the overlapping of NH of E59 and G60. The ambiguity due to overlapping of NH of T36 and G37 has been resolved by a NOESY experiment at 30°C. The positioning of NH of E107 was determined at 30°C in a NOESY experiment from the appearance of a long spin system exhibiting strong connectivities with two neighbouring residues (K106 and A108). E73, which exhibited only a weak $C^\alpha H$-NH correlation at 2.00 pm in the COSY and TOCSY experiments, was determined in the same way from the intense cross-peaks with D72 and E74. All the assignments were confirmed by a series of 2- and 3-dimensional heteronuclear HSQC-NOESY experiments using a ^{15}N-enriched sample. This assignment process is illustrated for the C-terminal helix in Fig. 3. The side-chain protons of three residues, Q1, G56, and N33, for which the amide proton resonances are not observable, were assigned as the remaining spin systems in the aliphatic part of the TOCSY, and were further confirmed by ^{13}C spectroscopy.

Assignment of Aromatic Side-Chains—In the DQF-COSY and TOCSY experiments at 45°C, correlations for the five Phe, four of the five Tyr, three His, and two Trp were observed, as shown in Fig. 4. The three aromatic rings of H19, H75, and H111 show narrow cross-peaks in the DQF-COSY and TOCSY experiments originating from the ^4J coupling constant between C(2)H and C(4)H. Connections with the assigned side-chains have been observed in the NOESY spectra in D_2O, in which NOEs between C(4)H with the β protons of the side-chains are observed. As in other large cytochromes *c*, C(2)H and C(4)H of histidine 19, which is coordinated to the iron of the heme, are strongly shifted upfield by about 7 ppm. The N_1H proton of H19 is also in slow exchange, suggesting that in solution it is involved in hydrogen bonding, probably, judging from the X-ray structure, with the carbonyl of P38 (*20*).

The ring protons of the two tryptophans (W71 and W114) have been assigned from their characteristic connectivities in the COSY and TOCSY experiments, and have been connected to the assigned NH-$C^\alpha H$-$C^\beta H_2$ segment *via* the TOCSY correlation between H(2) and N1H of the ring, and NOESY correlations between H(7) and N^1H, and H(2), and the $C\beta$ protons of the side-chain.

In DQF-COSY and TOCSY experiments, the ring protons of F12, F76, and F102 show the pattern characteristic of phenylalanine. The ring protons of F86 and F54 each give a single cross-peak in the DQF-COSY and TOCSY spectra. The five tyrosines give different coupling patterns. $H_{2,6}$ and $H_{3,5}$ of Y90 overlap, and have been identified using the NOESY correlation with $C^\beta H_2$. This assignment was confirmed in the 1-D NMR spectra of the cytochrome c_2 in D_2O by integration of the resonances. A similar case was encountered for Y41, but TOCSY cross-peaks between $H_{2,6}$ and $H_{3,5}$ remain visible due to the 0.03 ppm chemical shift difference. A single cross-peak, typical of tyrosine, is only

Downloaded from http://jb.oxfordjournals.org/ at Changhua Christian Hospital on October 2, 2012

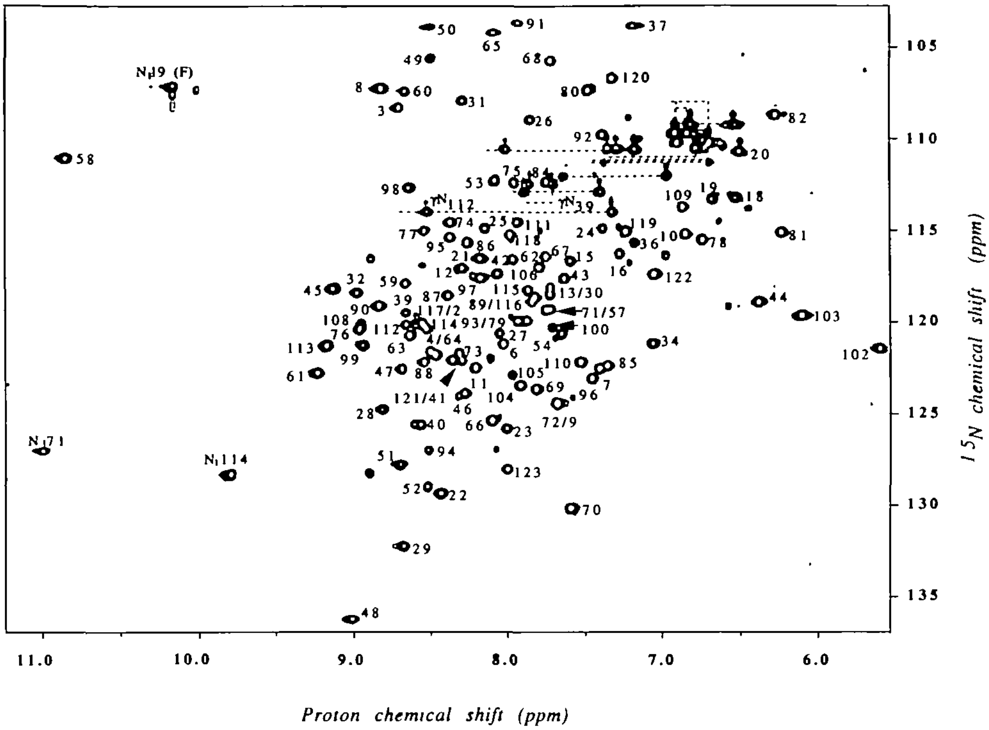

Fig. 2. **2D ^1H-^{15}N HSQC spectrum of *R. sphaeroides* ferrocytochrome c_2 uniformly labeled with ^{15}N.** The cross-peaks connected by dashed lines correspond to Gln and Asn side-chain NH_2 groups. (F) indicates folded peak.

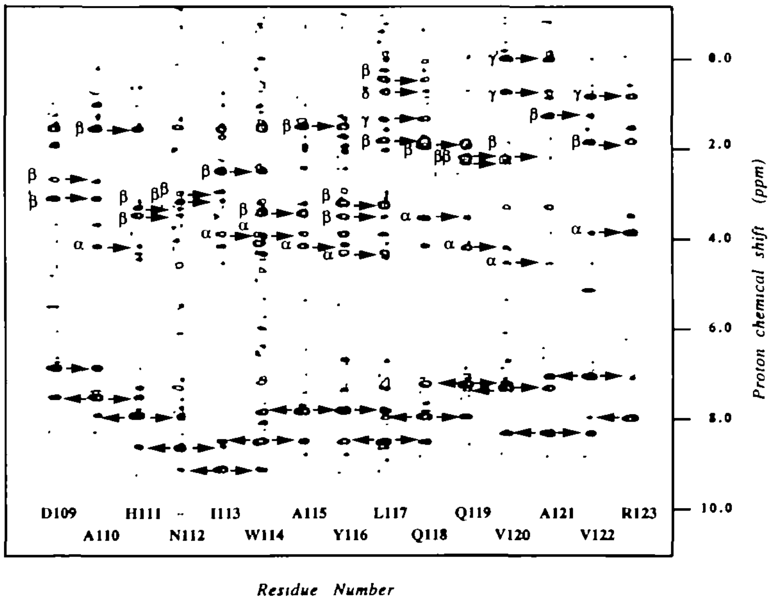

Fig. 3. **Amide strips extracted from the 150 ms mixing time 3D ^{15}N-edited NOESY-HSQC of *R. sphaeroides* ferrocytochrome c_2 for residues D109 to R123.** Selected intraresidue NOEs connecting NH to the H^{α}, H^{β}, H^{γ} protons are indicated by α, β, and γ, respectively, while interresidue connectivities are labeled with the residue corresponding to the site of originating magnetization.

observed for Y116. Interestingly, the ring protons of Y116 show a single cross-peak at 45°C, but a decrease in temperature to 25°C induces broadening of the correlation, indicating that the rate of rotation of the ring slows down on the NMR time scale. Y57 exhibits broad correlations at 45°C but becomes resolved at lower temperatures. The Y79 side chain shows four individual resonances, and one can conclude that the flipping rate of the ring is slower than 2,000 Hz, because one signal is shifted upfield to 3 ppm (see Fig. 1). Exchange relayed TOCSY cross-peaks were observed between H_5 and H_2, and also between H_6 and H_3.

Assignments of Long Side-Chains and Side-Chain $^1H^N$—Assignments of the long side-chains (Arg, Glu, Gln, Met, Lys, Leu, and Ile) are theoretically possible using the COSY correlations between the neighbouring protons. In fact, this is impeded for a protein of more than 100 residues by the numerous spectral overlaps and the peaks missing due to small J-coupling with respect to the line-width. We tried to overcome these difficulties using natural abundance ^{13}C spectroscopy, as previously described by Medvedeva *et al.* (*45*). Using two experiments (HSQC and TOCSY-HSQC), we have been able to assign all of the ^{13}C and ^1H methyl resonances, in particular the methyls of Ile and Leu, some of the β and γ protons of the glutamine or glutamate

Downloaded from http://jb.oxfordjournals.org/ at Changhua Christian Hospital on October 2, 2012

TABLE I. **^{1}H, ^{15}N, and ^{13}C resonance assignments of the ferrocytochrome *c*$_2$ of *Rhodobacter sphaeroides*** at 45°C and pH 6.7. [a] ^{1}H chemical shifts are referenced to the H_2O resonance at 4.582 ppm and are accurate to ±0.02 ppm. ^{15}N chemical shifts are referenced to $(^{15}NH_4)_2SO_4$ and are accurate to ±0.1 ppm. ^{13}C chemical shifts are referenced to TMS and are accurate to ±0.1 ppm. ^{13}C assignments are given in parentheses. [b] Unspecified proton assignments indicate proton resonances observed in the TOCSY spectra but not resolved in the COSY or HSQC spectra. [c] Assigned in the ^{1}H-^{13}C HSQC and HSQC-TOCSY experiments. [d] Assigned in a 2D-NOESY experiment at 300 K.

	Chemical shift (ppm)[a]				
Residue	^{15}N	NH	C$^{\alpha}$H	C$^{\beta}$H	Others[b]
Q1[c]	–	–	4.60 (57.6)	2.52, 2.07 (26.0)	C$^{\gamma}$H 2.42, 2.38 (30.1)
E2	120.1	8.53	4.41 (54.5)	2.10, 1.96 (28.6)	C$^{\gamma}$H 2.25, 2.08 (34.4)
G3	108.3	8.67	4.16, 3.71 (42.8)		
D4	121.8	8.51	5.20 (47.9)	2.74, 2.71 (40.9)	
P5		–	–	–	C$^{\delta}$H 3.94, 3.67 (48.8)
E6	121.2	8.04	4.15 (56.5)	2.10 (34.7)	C$^{\gamma}$H 2.33, 2.19
A7	122.6	7.43	4.17 (52.4)	1.48 (16.3)	
G8	107.2	8.81	3.93, 3.51 (44.7)		
A9	124.5	7.69	2.40 (52.6)	1.12 (16.6)	
K10	115.3	6.87	4.08	1.92	1.70; C$^{\gamma}$H 1.59, 1.46; C$^{\epsilon}$H 2.99
A11	122.6	8.21	4.44 (52.5)	1.65 (15.5)	
F12	117.2	8.31	4.55	3.23, 2.99	H$_{(2-6)}$ 7.35, H$_{(3-5)}$ 6.60, H$_{(4)}$ 6.07
N13	118.1	7.75	4.20	3.03, 2.8 (36.5)	
Q14	–	7.97	4.32	2.43	C$^{\gamma}$H 2.71, 2.78
C15	116.7	7.61	4.95 (52.5)	1.93, 1.15	
Q16	122.6	7.29	4.41	2.10	C$^{\gamma}$H 2.22, 2.05
T17	–	7.08	3.97 (62.5)	4.28 (67.7)	C$^{\gamma}$H$_3$ 1.51 (20.6)
C18	113.4	6.55	4.25	1.70, 0.68 (38.2)	
H19	113.4	6.69	3.39	1.10, 0.71 (29.1)	H$_{(2)}$ 0.43, H$_{(4)}$ 0.16, N$_{(1)}$H 10.15, ^{15}N$_{(1)}$ 166.9
V20	110.7	6.52	4.39	1.99	C$^{\gamma}$H$_3$ 0.77 (19.5), 0.52 (15.2)
I21	116.7	8.18	4.13 (60.4)	1.55 (37.4)	C$^{\gamma}$H 0.28, 1.18 (25.4), C$^{\gamma}$H$_3$ 0.63 (17.0), C$^{\delta}$H$_3$ −0.11 (11.9)
V22	129.4	8.44	4.62 (58.8)	1.59	C$^{\gamma}$H$_3$ 0.73 (19.8), 0.68 (18.3)
D23	125.8	8.01	2.66 (51.2)	2.54, 1.85 (38.1)	
D24	114.9	7.36	4.33	2.84, 2.62 (38.1)	
S25	114.9	8.16	4.51	3.93, 3.84 (62.2)	
G26	109.0	7.88	4.11, 3.34 (42.6)		
T27	120.6	8.07	3.97 (60.9)	3.95 (66.3)	C$^{\gamma}$H$_3$ 0.95 (19.6)
T28	124.8	8.79	4.00	3.98 (66.2)	C$^{\gamma}$H$_3$ 0.87 (19.8)
I29	132.2	8.67	3.81 (60.4)	1.44 (36.1)	C$^{\gamma}$H 1.32, 1.13 (26.6), C$^{\gamma}$H$_3$ 0.78 (14.7), C$^{\delta}$H$_3$ 0.77 (11.9)
A30	118.6	7.74	4.54 (49.9)	1.30 (20.6)	
G31	107.9	8.30	4.41, 3.67 (43.0)		
R32	118.5	8.96	4.47 (53.3)	1.78, 1.53 (28.4)	C$^{\gamma}$H 1.48 (2.50), C$^{\delta}$H 3.13 (41.5)
N33	–	–	4.22	2.60, 2.87 (36.3)	
A34	121.3	7.07	4.06 (51.2)	0.81 (18.3)	
K35		8.22	4.35	1.96	1.55, C$^{\gamma}$H 1.30, 1.25, C$^{\epsilon}$H 2.9
T36	115.6	7.20	4.03 (63.9)	4.04 (67.7)	C$^{\gamma}$H$_3$ 1.88 (20.9)
G37	103.5	7.20	3.44, −0.53 (38.8)		
P38	–				
N39	119.6	8.63	4.04	2.82, 2.69 (35.3)	N$^{\gamma}$H$_2$ 7.86, 7.71, ^{15}N 112.5
L40	125.7	8.58	3.89 (51.9)	1.09, 0.98 (39.4)	C$^{\gamma}$H 0.96 (23.5), C$^{\delta}$H$_3$ −0.62 (18.7), −1.06 (21.8)
Y41	122.1	8.31	3.63	2.58, 2.52	6.78, 6.81
G42	117.4	8.06	3.89, 3.44 (43.5)		
V43	117.6	7.64	3.71	1.99	C$^{\gamma}$H$_3$ 1.21 (22.1), 0.80 (19.1)
V44	118.9	6.38	3.69	1.69	C$^{\gamma}$H$_3$ 0.92 (18.5), −0.05 (17.7)
G45	118.2	9.14	4.31, 3.72 (43.7)		
R46	123.9	8.28	4.39		2.30, 2.14, 1.79, 2.09, 2.16
T47	122.5	8.65	4.47 (61.9)	3.90 (66.8)	C$^{\gamma}$H$_3$ 1.26 (19.9)
A48	135.9	9.010	4.47 (51.7)	1.07 (16.9)	
G49	105.6	8.52	3.31, 2.08 (44.6)		
T50	103.5	8.34	4.76 (59.4)	4.55 (69.5)	C$^{\gamma}$H$_3$ 1.02 (19.0)
Q51	127.6	8.69	4.32	2.66	C$^{\gamma}$H 2.80 2.50
A52	129.1	8.50	4.06 (53.9)	1.50 (17.5)	
D53	112.4	8.09	4.69 (51.4)	2.82, 2.74 (39.4)	
F54	120.8	7.67	4.66 (54.1)	3.04, 2.96	6.96, 7.65
K55	–	–			
G56[c]	–	–	4.35, 3.11 (44.9)		
Y57	119.3	7.67	5.77 (57.7)	3.66, 3.10	H$_{(2-6)}$ 8.88, 7.63, H$_{(3-5)}$ 7.34, 7.39 (at 303 K)
G58	111.1	10.84	4.64, 4.48 (42.4)		
E59	118.0	8.65	4.08 (57.8)	2.19, 2.11 (27.4)	C$^{\gamma}$H 2.49 (35.0)
G60	107.4	8.65	4.04, 3.51 (44.6)		
M61	122.8	9.23	4.48	2.68, 2.57 (29.4)	2.35, C$^{\epsilon}$H$_3$ 2.64 (17.5)
K62	116.7	8.00	3.99		2.02, 1.95, 1.62, C$^{\gamma}$H 1.80, C$^{\epsilon}$H 3.10, 3.03
E63	120.8	8.62	4.16 (54.8)	2.35, 2.20 (27.0)	C$^{\gamma}$H 2.47, 2.35 (33.6)
A64	121.7	8.47	3.94 (53.9)	1.30 (15.2)	

Downloaded from http://jb.oxfordjournals.org/ at Changhua Christian Hospital on October 2, 2012

TABLE I. (Continued)

	Chemical shift (ppm)^{a}				
Residue	^{15}N	NH	C$^{\alpha}$H	C$^{\beta}$H	Others^{b}
G65	104.1	8.00	4.38, 4.00 (45.7)		
A66	125.3	8.10	4.15 (52.6)	1.55 (15.8)	
K67	116.5	7.77	4.27	2.17, 1.97	1.69, 1.56, C$^{\epsilon}$H 2.96
G68	105.8	7.73	4.41, 3.62 (42.9)		
L69	123.6	7.83	3.63 (54.7)	0.82, 0.6 (38.1)	C$^{\gamma}$H −0.10 (24.4), C$^{\delta}$H$_3$ −0.23 (24.7), −0.22 (19.3)
A70	130.2	7.59	4.68 (47.5)	1.06 (18.6)	
W71	119.4	7.76	4.54	3.45, 4.20 (27.3)	N$_{(1)}$H 10.99, ^{15}N$_{(1)}$ 127.19, H$_{(2)}$ 7.43, H$_{(4)}$ 7.44, H$_{(5)}$ H$_{(6)}$ 6.36, H$_{(7)}$ 7.38
D72	124.5	7.70	4.93 (49.3)	3.22, 2.96	
E73	121.7	8.35	2.04 (58.8)		2.18, 1.66, 1.31
E74	114.6	8.34	3.82 (57.7)	1.70 (27.6)	C$^{\gamma}$H 2.05 1.95 (34.1)
H75	112.6	8.00	4.42	3.25, 3.09 (26.7)	H$_{(2)}$ 8.58, H$_{(4)}$ 7.35
F76	120.5	8.96	4.17	3.01, 2.91	H$_{(2-6)}$ 7.16, H$_{(3-5)}$ 8.12, H$_{(4)}$ 7.80
V77	115.1	8.54	3.26 (64.1)	1.96	C$^{\gamma}$H$_3$ 0.68 (19.8), 0.57 (18.7)
Q78	115.6	6.77	3.90 (56.3)	2.27, 2.13 (27.8)	C$^{\gamma}$H 2.63, 2.43 (32.0)
Y79	120.0	7.87	3.32	2.33, 1.83	H$_{(2-6)}$ 5.54, 6.92, H$_{(3-5)}$ 3.30, 6.24
V80	107.5	7.49	2.01 (61.4)	1.24	C$^{\gamma}$H$_3$ 0.50 (18.4), 0.13 (19.7)
Q81	115.2	6.26	4.13		1.72, 2.35, 1.99, 1.94
D82	108.8	6.29	3.82	2.74, 2.63 (38.0)	
P83	–	–	3.39	1.11	C$^{\gamma}$H 0.38, −0.51 (23.6), C$^{\delta}$H 2.86, 2.61 (48.6)
T84	112.3	7.73	3.65	4.07 (66.4)	C$^{\gamma}$H$_3$ 1.26 (20.5)
K85	122.4	7.39	3.66		1.60, 1.47, 1.32, 1.22, C$^{\epsilon}$H 2.85
F86	115.7	8.27	4.14	3.25, 3.11	7.23, 6.84
L87	118.6	8.38	3.90 (51.9)	1.95, 1.03 (40.7)	C$^{\gamma}$H 2.30, C$^{\delta}$H$_3$ 0.94 (20.4)
K88	122.2	8.54	3.99		1.85, 1.63, 1.58, 1.46, C$^{\epsilon}$H 2.84, 2.97
E89	118.7	7.84	3.83 (56.9)	1.96, 1.87 (27.3)	C$^{\gamma}$H 2.36, 2.11 (34.7)
Y90	119.1	8.84	3.69	2.24	H$_{(2-6)}$ and H$_{(3-6)}$ 6.91
T91	103.2	7.86	3.83	4.24 (68.7)	C$^{\gamma}$H$_3$ 1.41 (20.5), (OH) 4.94
G92	109.8	7.41	4.01, 3.66 (43.9)		
D93	120.0	7.94	4.70 (50.1)	3.09, 2.41	
A94	127.0	8.50	3.94 (52.2)	1.42 (16.5)	
K95	115.4	8.39	4.25	1.88	1.44, 1.40, C$^{\delta}$H 1.67, C$^{\epsilon}$H 3.00
A96	123.1	7.46	4.07 (51.2)	1.24 (16.8)	
K97	117.6	8.15	4.54		1.76, 1.67, 1.38, C$^{\epsilon}$H 2.99
G98	112.6	8.62	4.08, 3.32 (43.9)		
K99	121.3	8.94	4.37		2.46, 2.05, 1.99, 1.66, C$^{\epsilon}$H 3.27, 3.19 (40.1)
M100	120.3	7.70	3.32	−0.17, −1.39	C$^{\gamma}$H −2.67, −3.57, C$^{\epsilon}$H$_3$ −2.95 (12.8)
T101	–	7.95	3.74 (59.0)	4.33 (65.7)	C$^{\gamma}$H$_3$ 1.26 (22.4)
F102	121.5	5.64	3.95	2.92, 1.21 (40.1)	H$_{(2-6)}$ 6.92, H$_{(3-5)}$ 7.42, H$_{(4)}$ 7.62
K103	119.7	6.11	3.65	1.15, 1.02 (32.6)	C$^{\gamma}$H 0.81, 0.70 (22.5), C$^{\delta}$H 1.38, C$^{\epsilon}$H 2.68 (39.9)
L104	123.4	7.92	4.16 (51.2)	1.41, 0.93 (41.8)	C$^{\delta}$H$_3$ 1.14 (19.6), 0.94 (24.6), C$^{\gamma}$H 1.55
K105	122.9	7.98	4.08		1.61, 1.41, 1.32, 1.08, C$^{\epsilon}$H 2.93
K106	117.1	7.76	4.54		1.88, 1.79, 1.52, 1.39, C$^{\epsilon}$H 2.98
E107^{d}	–	8.96	3.62		2.19, 2.01, 1.85
A108	120.1	8.92	4.28 (53.9)	1.48 (16.3)	
D109	113.8	6.90	4.58	3.03, 2.63 (38.9)	
A110	122.2	7.55	4.13 (53.8)	1.48 (17.5)	
H111	114.6	7.95	4.42	3.43, 3.25 (26.2)	H$_{(2)}$ 8.70, H$_{(4)}$ 7.32
N112	120.1	8.66	4.50	3.13, 2.89 (34.3)	N$^{\gamma}$H$_2$ 8.54, 7.35, ^{15}N 114.0
I113	121.3	9.17	3.85	2.43	C$^{\gamma}$H 2.46, 1.52, C$^{\gamma}$H$_3$ 1.66 (17.5), C$^{\delta}$H$_3$ 1.45 (13.9)
W114	120.5	8.54	3.8	3.41, 3.34 (26.8)	N$_{(1)}$H 9.79, ^{15}N$_{(1)}$ 128.31, H$_{(2)}$ 7.08, H$_{(7)}$ 7.52, H$_{(6)}$ 7.13, H$_{(5)}$ 6.41, H$_{(4)}$ 5.75
A115	118.4	7.89	4.11 (53.0)	1.42 (15.2)	
Y116	118.7	7.85	4.27	3.46, 3.17 (36.3)	H$_{(2-6)}$ 6.91, H$_{(3-5)}$ 6.24
L117	120.1	8.56	3.25 (55.4)	1.27, 0.38 (37.8)	C$^{\gamma}$H 1.74 (23.6), C$^{\delta}$H$_3$ 0.64 (24.7), 0.15 (20.2)
Q118	115.3	8.00	3.49 (56.4)	1.89, 1.85 (26.9)	C$^{\gamma}$H 1.89, 1.74 (32.7)
Q119	115.1	7.25	4.18 (55.8)	2.21, 2.12 (27.8)	C$^{\gamma}$H 2.42, 2.28 (32.1)
V120	106.8	7.34	4.50	2.13	C$^{\gamma}$H$_3$ 0.63 (18.8), −0.10 (14.8)
A121	122.1	8.36	4.57 (48.3)	1.18 (18.3)	
V122	117.3	7.05	3.83 (59.1)	1.78	C$^{\gamma}$H$_3$ 0.75 (19.5), 0.73 (19.1)
R123	127.9	7.99	4.64 (51.6)	1.75, 1.46 (29.1)	1.58, C$^{\delta}$H 3.29, 3.23 (41.4); N$^{\epsilon}$H 8.82
P124	–	–			C$^{\delta}$H 4.20, 3.94 (49.2)

residues, and about 70% of the ^{13}C$^{\alpha}$. In the case of the ^{13}C$^{\alpha}$, assignments were made from the coherence transfer in the TOCSY-HSQC experiment or from the HSQC when the ^{1}H$^{\alpha}$ chemical shift was unambiguous. However, even with the dispersion that the ^{13}C caused, we could not assign many proton resonances of the long residues, in particular the lysine residues for which ^{13}C and ^{1}H are located in a crowded region of the spectra. Complete assignment of the long chain residues would require in our case the use of a 100% ^{13}C-enriched protein with heteronuclear spectroscopy, as described by Caffrey *et al.* (*49*) for the ^{13}C assignment of the *R. capsulatus* ferrocytochrome c_2.

Downloaded from http://jb.oxfordjournals.org/ at Changhua Christian Hospital on October 2, 2012

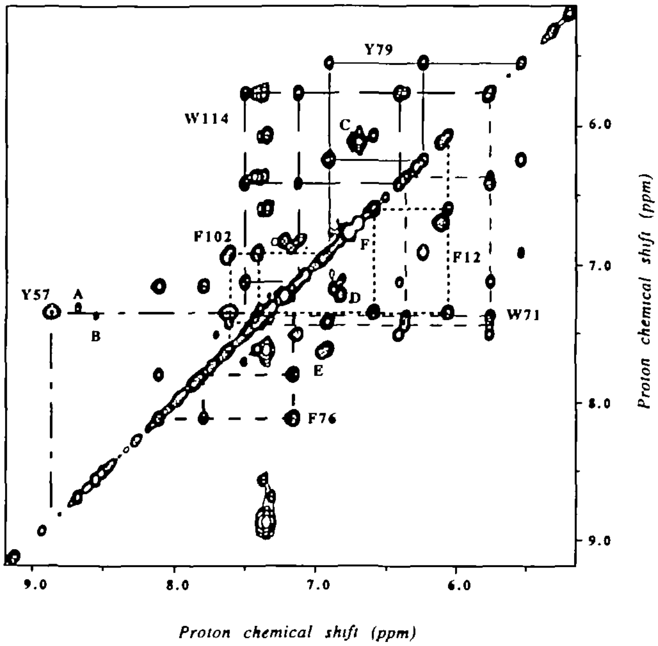

Fig. 4. **Aromatic (F2)-aromatic (F1) section of a TOCSY spectrum of *R. sphaeroides* ferrocytochrome c_2 acquired with an isotropic mixing time of 80 ms, in D_2O at 45°C and pH 6.7.** Connectivities are indicated above the diagonal for Y57, Y79, F102, and W114, and below the diagonal for F12, W71, and F76. Single cross-peaks are indicated for (A) H111, (B) H75, (C) Y116, (D) F86, (E) F54, and (F) Y41. An additional connectivity between the protons of Y79 and a resonance at 3.03 ppm is shown in Fig. 1.

In the HSQC-^{15}N spectrum, all the correlations expected for the 11 amide side-chains of the 7 glutamines and the 4 asparagines are observed (see Fig. 2). However, the NOE correlations were not sufficiently strong enough to allow unambiguous assignments, except for the side-chain NH of N39 and N112.

Heme Assignments—The heme resonances were identified following the procedure described by Keller and Wüthrich (*54*). The values are presented in Table II and the heme proton numbering is indicated in Fig. 5. The protons of propionates 13 and 17 were assigned in the 2D NOESY experiments from the observation of strong NOESY cross-peaks with the γ proton of the heme. These assignments were further confirmed in the ^{13}C HSQC experiment by the presence of a pair of CH correlations at a ^{13}C chemical shift similar to those reported by Caffrey *et al.* (*49*), and Medvedeva *et al.* (*45*).

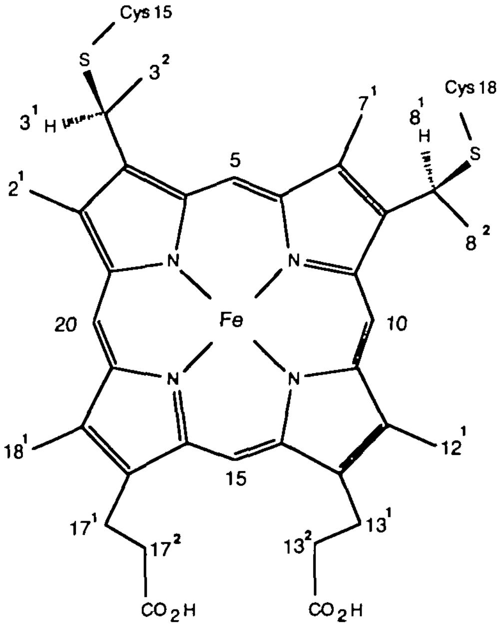

Fig. 5. **Structure of the covalently bonded heme group in the *R. sphaeroides* ferrocytochrome c_2.** The nomenclature used for the heme protons is according to the IUPAC recommendations.

TABLE II. **^{1}H and ^{13}C resonance assignments of the heme group of the *Rhodobacter sphaeroides* ferrocytochrome c_2 at 45°C and pH 6.7.** ^{1}H chemical shifts are referenced to the H_2O resonance at 4.582 ppm and are accurate to ±0.02 ppm. ^{13}C chemical shifts are referenced to TMS and are accurate to ±0.1 ppm. Heme protons are named following the IUPAC recommendations (see Fig. 5).

	Chemical shift (ppm)^a	
Nucleus	^{1}H	^{13}C
5-*meso*	9.16	—
10-*meso*	9.67	—
15-*meso*	9.70	—
20-*meso*	9.45	—
Methyl-2^1	3.92	14.0
Methyl-7^1	3.28	13.4
Methyl-12^1	3.54	11.5
Methyl-18^1	2.49	10.1
Thiomethyl-3^2	2.23	24.1
Thiomethine-3^1	5.32	33.2
Thiomethyl-8^2	2.37	20.7
Thiomethine-8^1	6.29	36.3
Propionate-13^1	4.19	23.2
Propionate-13^2	3.61, 2.72	45.1
Propionate-17^1	4.4, 3.75	22.9
Propionate-17^2	3.75, 2.88	42.4

Secondary Structure Determinations—In NMR studies on proteins, helices are characterized by the presence of consecutive $d_{NN(i,i+1)}$ and $d_{\alpha N(i,i+3)}$ connectivities, and $^3J(HC^{\alpha}NH)$ coupling constants that are less than 6 Hz (*55*). In Fig. 6, the sequential connectivities that were observed in the NOESY-HSQC 3D or homonuclear 2D NOESY experiments are presented. In addition, the $^3J(HC^{\alpha}NH)$ coupling constants, which were calculated from the relative intensities of the HC^{α}-NH cross- and diagonal peaks in the HNHA 3D experiment (*46*), are presented. Together, the sequential connectivities and $^3J(HC^{\alpha}NH)$ coupling constants suggest that there are five helical regions in *R. sphaeroides* ferrocytochrome c_2: residues 6-16, 60-68, 74-82, 84-91, and 109-120. The occurrence of $d_{\alpha N(i,i+2)}$ suggests that the first helix deviates from the canonical α-helix structure, a feature observed in other cytochromes *c* (*56*). No other regular secondary structure could be determined. In Fig. 7, "amide strips" extracted in a 3D HSQC-NOESY experiment are presented for the assignment of residues 20 to 32. For these residues, X-ray diffraction results indicate the presence of an irregular antiparallel β-loop stabilized by four hydrogen bonds (*20*).

DISCUSSION

In this paper, we report the quasi-complete assignment of the proton and ^{15}N resonances of the ferrocytochrome c_2 of

Downloaded from http://jb.oxfordjournals.org/ at Changhua Christian Hospital on October 2, 2012

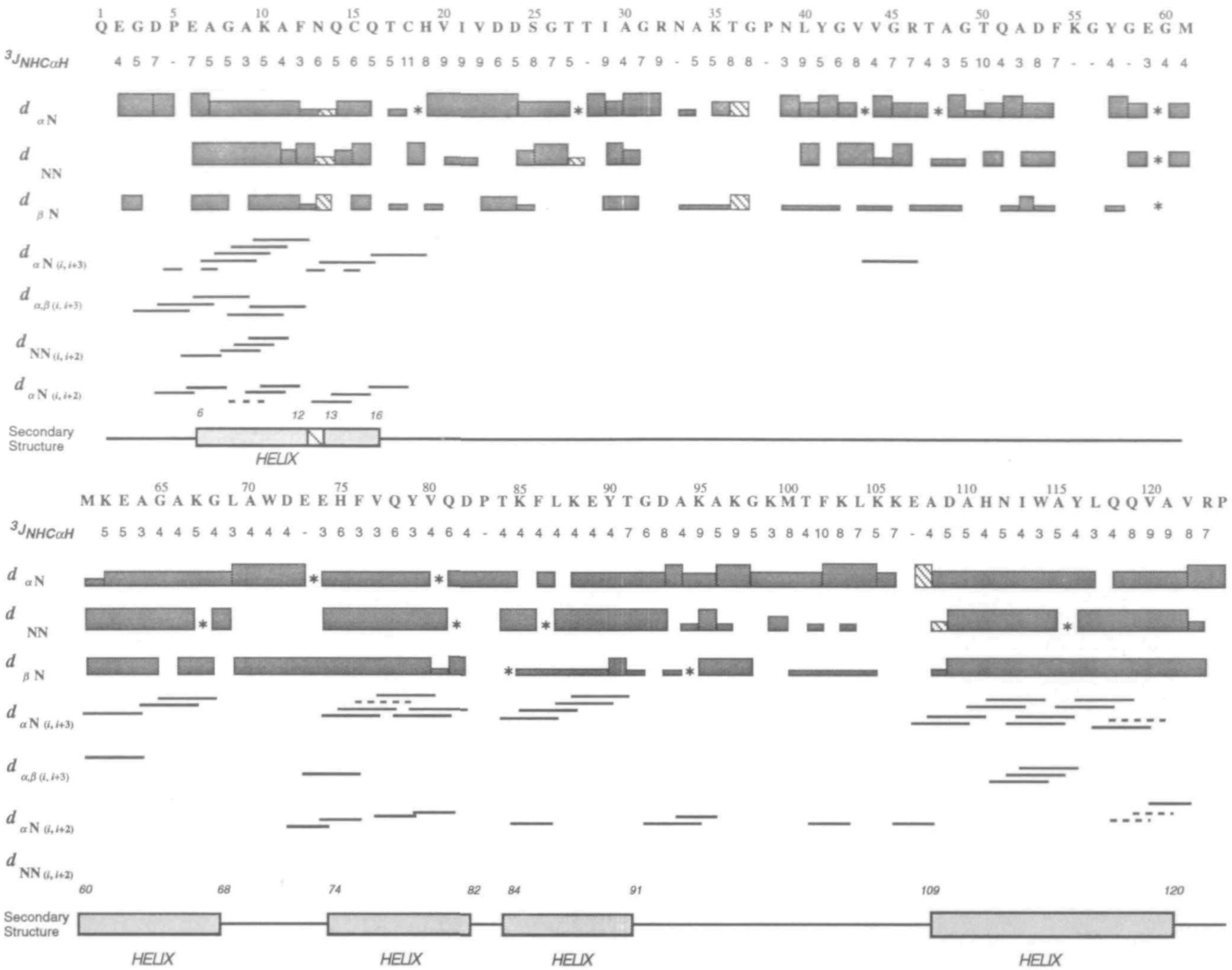

Fig. 6. **Secondary structure determination of *R. sphaeroides* ferrocytochrome c_2.** A summary of the $^3JH^NH^\alpha$ values determined in a 3D-HNHA experiment, and of the sequential and short range NOEs (i to $<i+4$) observed in the ^{1}H-^{1}H NOESY and ^{1}H-^{15}N NOESY-HSQC spectra. Spectra were acquired with a mixing time of 150 ms in H_2O at 45°C and pH 6.7. The $^3JH^NH^\alpha$ coupling constants are listed in units of Hz and are accurate to ±1 Hz. The NOE have been grouped into three categories, strong, medium, and weak, which is reflected by the bar height. Asterisks indicate peaks which could not be discriminated because of degenerate resonance frequencies. Hatched bars indicate NOE correlations observed at 300 K. For the proline residues, correlations are indicated when NOE interactions were observed between the δ protons of the proline and the α proton of the preceeding residue.

R. sphaeroides. Due to its molecular mass of 14 kDa, the cytochrome c_2 of *R. sphaeroides* fell in the upper limits for the classical NMR sequential assignment method based on 2D proton-proton correlation spectroscopy (*55*). However, the classical strategy has been found to be effective in our case, and heteronuclear ^{15}N NMR was eventually used only to extend and corroborate the assignments. The major difficulties in the assignment process occurred for residues expected to be on the surface of the cytochrome and thus exposed to the solvent, in particular, for NH of residues N33, K55, and G56, which could not be observed. We have nevertheless been able to assign, at least partially, all the residues, except Pro 38 and Lys 55. Completion of the assignments using ^{13}C-labeling of the protein together with heteronuclear spectroscopy as described for the *R. capsulatus* cytochrome c_2 (*49*) is under way.

Although this work was only a first step toward elucidation of the three-dimensional structure in solution and the characterization of the dynamic properties of the protein, some preliminary insights into the global fold of the protein can be made. As expected, the global 3D fold of the cytochrome c_2 of *R. sphaeroides* in solution is not different from that determined by X-ray crystallography (*20*). We observed the presence of five helices at positions 6-16, 60-68, 74-82, 84-91, and 109-120, in fair agreement with those observed in the crystal structure, taking into account that the positioning of the beginning and the end of helices is within one residue. The beginning of the N-terminal helix was placed at E6 on the basis of the coupling constants and the observation of a strong $d_{\alpha N}$ between E6 C^αH and A7 NH; nevertheless, the presence of medium-range NOEs between D4 C^αH, and the E6, A7, and G8 NH suggests that segment 4-7 adopts a loop conformation. In the crystal structure, the third helix and the C-terminal helix have been found to begin at residues 72 and 107, respectively. In solution, the absence of observable d_{NN} correlations, to-

Downloaded from http://jb.oxfordjournals.org/ at Changhua Christian Hospital on October 2, 2012

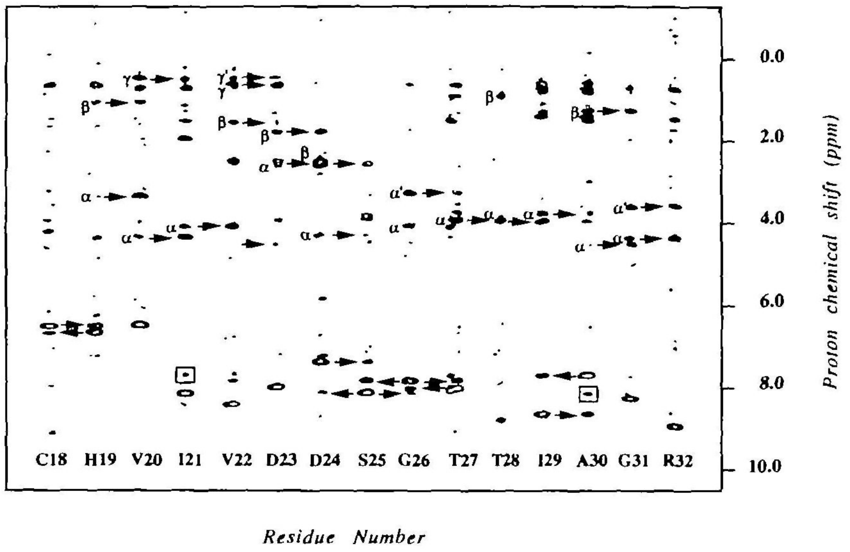

Fig. 7. **Amide strips extracted from the 150 ms mixing time 3D ^{15}N-edited NOESY-HSQC of *R. sphaeroides* ferrocytochrome c_2 for residues V20 to R32.** Selected intraresidue NOEs connecting NH to the H^{α}, H^{β}, and H^{γ} protons are indicated by α, β, and γ, respectively, while interresidue connectivities are labeled with the residue corresponding to the site of originating magnetization. Boxed correlations indicate long-range interactions between the amide protons of I21 and A30.


SP: QEGDPEAGAKAFNQCQTCHV IVDDSGTTIAGRNAKTGPNLY GVV
DE: QDGDAAKGEKEFNKCKACHM IQAPDGTDII-KGGKTGPNLY GVV
CA: GDAAKGEKEFNKCKTCHS IIAPDGTEIV-KGAKTGPNLY GVV

SP: GRTAGTQADFKGYGEGMKEAGA--KGLAWDEEHFVQYVQDPT
DE: GRKIASEEGFK-YGEGILEVAEKNPDLTWTEADLIEYVTDPK
CA: GRTAGTYPEFK-YKDSIVALGA--SGFAWTEEDIATYVKDPG

SP: KFLKEYTGDAKAKGKMTFKLKKEADAHNIWAYLQQVAVRP
DE: PWLVKMTDDKGAKTKMTFKMGKNQA--NVVAFLAQNSPDAGGDGGEAA
CA: AFLKEKLDDKKAKTGMAFKLAKGGE--DVAAYLASVVK

Fig. 8. **Sequence alignment of the three class I cytochromes *c* of *R. sphaeroides*, *P. denitrificans*, and *R. capsulatus*.** SP: *R. sphaeroides* cytochrome c_2, DE: *P. denitrificans* cytochrome c_{551}, CA: *R. capsulatus* cytochrome c_2. Hatched bars indicate the positions of the helices, as determined in NMR studies (this work; *49, 52*). Grey squares indicate the locations of the helices, as determined in X-ray crystallography studies (*20, 21, 58*). The sequence alignment was made following Moore and Pettigrew (*56*).

gether with the observation of strong $d_{\alpha N}$ correlations between residues 72 and 73, and 107 and 108, led us to place the beginning of these helices at two residues later than the crystal structure. In agreement with the known structures of cytochromes *c* (*56*), we observed several NOEs between the residues of the C-terminal and N-terminal helices, for example, between G8 and Y116, and G8 and N112. The ring protons of F12 and Y116 are in close contact, as the conserved aromatic residues are always in the N- and C-terminal helices. Furthermore, the rotation of either of these rings is frequently sterically hindered in cytochromes *c* (see, for instance, Ref. *57*), and the broadening of the Y116 ring resonances upon a decrease in temperature is not an exception to the rule. We did not observe alternative upfield and downfield shifts of H^{α}, which are characteristic of a β sheet conformation, for segment 20–30. Strong NH-NH correlations between I29 and A30 are also not in favor of an extended conformation for these residues. Apart from contact between NH of residues 21 and 30, no other NOE interactions could be observed between NH of the residues of this loop, a result indicative of the presence in solution of an Ω loop conformation, as described for the *R. capsulatus* cytochrome c_2 (*52*).

The crystal structures of two homologous large cytochromes: the cytochrome c_2 of *R. capsulatus* and the cytochrome c_{550} of *P. denitrificans*, were previously determined (*21, 22, 58*). These cytochromes share 57% sequence identity, and 53 and 51% with the *R. sphaeroides* cytochrome c_2, respectively (*56*). The locations of the secondary structure elements are shown in Fig. 8. The positions of the helices indicate a very similar global structure of these three molecules. The structural homology with the *R. capsulatus* cytochrome c_2 was also confirmed at the atomic level by the observation of similar chemical shifts for the protons of some homologous residues. For example, we observed the same shielding or deshielding of the structurally-sensitive $C^{\alpha}H$ of Ala 9, Asp 23, Gly 37, Tyr 57, and Val 80 as that observed for $C^{\alpha}H$ of the homologous Glu 7, Ala 21, Gly 34, Tyr 53, and Val 76 of the cytochrome c_2 of *R. capsulatus*. In the same way, the

Downloaded from http://jb.oxfordjournals.org/ at Changhua Christian Hospital on October 2, 2012

NH chemical shifts of G58, F102, and K103 are similar to those of the homologous K54, F98, and K99 of the *R. capsulatus* cytochrome c_2. Last, one of the ring protons of Y79 is shielded by about 4 ppm, similar to the equivalent proton of Y75 of *R. capsulatus* (*52*). This conclusion can be extended to the dynamic properties of these two cytochromes, as we observed similar flipping rates for the aromatic rings of homologous tyrosine residues. The aromatic ring of Y116 of *R. sphaeroides* cytochrome c_2 showed a slow flipping rate on the NMR time scale, like that of the homologous Y110 of *R. capsulatus* cytochrome c_2; the broadening of the Y79 and Y57 ring resonances observed when the temperature was decreased indicates an intermediate flipping rate, a feature also observed for the homologous Y76 and Y55 of *R. capsulatus* (*52*).

Finally, the *R. sphaeroides* cytochrome c_2 clearly shows broader signals and poorer coherence transfer than other medium or large cytochromes *c* under similar experimental conditions. One may speculate that this behavior originates from the acidic isoelectric point, 5.5, and the low net charge, +2, of the *R. sphaeroides* cytochrome c_2 (*59*). Accordingly, more hydrophobic contact may be possible between two molecules under the NMR experimental conditions (*i.e.* a $\mathrm{pH}<6.5$) than the *R. capsulatus* cytochrome c_2 or the horse cytochrome *c*, for which the pI and net charge are higher, 7.1 and +3, and about 10 and +8, respectively (*59*). Such a hypothesis implies that the electron self exchange rate parameter would be different for the *R. sphaeroides* cytochrome c_2 from that observed for the other cytochromes *c*, a point under investigation.

We wish to thank Drs. E. Forest and Y. Petillot for their help in the mass spectroscopy analysis.

REFERENCES

1. Prince, R.C. (1990) Bacterial photosynthesis: From photons to Δp in *Bacterial Energetics. The Bacteria* (Krulwich, T.A., ed.) Vol. 12, pp. 111-150, Academic Press, New York
2. Baccarini-Melandri, A., Jones, O., and Hauska, G. (1978) Cytochrome c_2, an electron carrier shared by the respiratory and photosynthetic electron transport chain of *Rhodopseudomonas capsulata*. *FEBS Lett.* **86**, 151-153
3. Ferguson, S.T., Jackson, J.B., and McEwan, A.G. (1987) Anaerobic respiration in the *Rhodospirillaceae*: Characterisation of the pathways and evaluation of roles in redox balancing during photosynthesis. *FEMS Microbiol. Rev.* **46**, 117-143
4. Vermeglio, A. and Carrier, J.-M. (1984) Photoinhibition by flash and continuous light of oxygen uptake by intact photosynthetic bacteria. *Biochim. Biophys. Acta* **764**, 233-238
5. Richaud, P., Marrs, B.L., and Vermeglio, A. (1986) Two modes of interaction between photosynthetic and respiratory electron chains in whole cells of *Rhodopseudomonas capsulata*. *Biochim. Biophys. Acta* **850**, 256-263
6. Sabaty, M., Gans, P., and Vermeglio, A. (1993) Inhibition of nitrate reduction by light and oxygen in *Rhodobacter sphaeroides* forma sp. *denitrificans*. *Arch. Microbiol.* **159**, 153-159
7. Tiede, D.M. and Dutton, P.L. (1993) Electron transfer between bacterial reaction centers and mobile *c*-type cytochromes in *The Photosynthetic Reaction Centers* (Deisenhofer, J. and Norris, J.R., eds.), pp. 257-288, Academic Press, New York
8. Allen, J.P., Feher, G., Yeates, T.O., Rees, D.C., Deisenhofer, J., Michel, H., and Huber, R. (1986) Structural homology of reaction centers from *Rhodobacter sphaeroides* and *Rhodopseudomonas viridis* as determined by X-ray diffraction. *Proc. Natl. Acad. Sci. USA* **83**, 8589-8593
9. Allen, J.P., Feher, G., Yeates, T.O., Komiya, H., and Rees, D.C. (1987) Structure of the reaction center from *Rhodobacter sphaeroides* R-26. The protein subunits. *Proc. Natl. Acad. Sci. USA* **84**, 6162-6166
10. Overfield, R.E. and Wraight, C.A. (1980) Oxidation of cytochrome *c* and c_2 by bacterial photosynthetic reaction centers in phospholipid vesicles. 1. Studies with neutral membranes. *Biochemistry* **19**, 3322-3327
11. Moser, C.C. and Dutton, P.L. (1988) Cytochrome *c* and c_2 binding dynamics and electron transfer with photosynthetic protein and other integral membrane redox proteins. *Biochemistry* **27**, 2450-2461
12. Venturoli, G., Mallardi, A., and Mathis, P. (1993) Electron transfer from cytochrome c_2 to the primary donor of *Rhodobacter sphaeroides* reaction centers. A temperature dependance study. *Biochemistry* **32**, 13245-13253
13. Wang, S., Li, X., Williams, J.C., Allen, J.P., and Mathis, P. (1994) Interaction between cytochrome c_2 and reaction centers in purple bacteria. *Biochemistry* **33**, 8306-8312
14. Joliot, P., Vermeglio, A., and Joliot, A. (1989) Evidence for supercomplexes between reaction centers, cytochrome c_2 and cytochrome bc_1 complex in *Rhodobacter sphaeroides* whole cells. *Biochim. Biophys. Acta* **975**, 336-345
15. Vermeglio, A., Joliot, P., and Joliot, A. (1993) The rate of cytochrome c_2 photooxidation reflects the subcellular distribution of reaction centers in *Rhodobacter sphaeroides*. *Biochim. Biophys. Acta* **1183**, 352-360
16. Sabaty, M., Jappe, J., Olive, J., and Vermeglio, A. (1994) Organization of electron transfer components in *Rhodobacter sphaeroides* forma sp. *denitrificans* whole cells. *Biochim. Biophys. Acta* **1187**, 313-323
17. Tiede, D.M. and Chang, C.H. (1988) The cytochrome-*c* binding surface of reaction centers from *Rhodobacter sphaeroides*. *Isr. J. Chem.* **28**, 183-191
18. Caffrey, M., Bartsch, R.G., and Cusanovich, M. (1992) Study of the cytochrome c_2-reaction center interaction by site-directed mutagenesis. *J. Biol. Chem.* **267**, 6317-6321
19. Tiede, D.M., Vashishta, A.-C., and Gunner, M.R. (1993) Electron-transfer kinetics and electrostatic properties of the *Rhodobacter sphaeroides* reaction center and soluble *c*-cytochromes. *Biochemistry* **32**, 4515-4531
20. Axelrod, H.E., Feher, G., Allen, J.P., Chirino, A.J., Day, M.D., Hsu, B.T., and Rees, D.C. (1994) Crystallization and X-ray structure determination of cytochrome c_2 of *Rhodobacter sphaeroides* in three crystal forms. *Acta Cryst. Section D.* **50**, 596-602
21. Benning, M., Wesenberg, G., Caffrey, M., Bartsch, R., Meyer, T., Cusanovich, M., Rayment, I., and Holden, H. (1991) Molecular structure of the cytochrome c_2 isolated from *Rhodobacter capsulatus* determined at 2.5 Å resolution. *J. Mol. Biol.* **220**, 673-685
22. Timkovich, R. and Dickerson, R.E. (1976) The structure of *Paracoccus denitrificans* cytochrome c_{550}. *J. Biol. Chem.* **251**, 4033-4046
23. Hall, J., Zha, X., Durham, B., O'Brien, P., Vieira, B., Davis, D., Okamura, M., and Millett, F. (1987) Reaction of cytochromes *c* and c_2 with the *Rhodobacter sphaeroides* reaction center involves the heme crevice device. *Biochemistry* **26**, 4494-4500
24. Hall, J., Kriaucionas, A., Knaff, D., and Millett, F. (1987) The reaction domain on *Rhodospirillum rubrum* cytochrome c_2 and horse cytochrome *c* with the *Rhodospirillum rubrum* cytochrome bc_1 complex. *J. Biol. Chem.* **262**, 14005-14009
25. Güner, S., Willie, A., Millett, F., Caffrey, M., Cusanovich, M., Robertson, D., and Knaff, D. (1993) The interaction between cytochrome c_2 and the cytochrome bc_1 complex in the photosynthetic purple bacteria, *Rhodobacter capsulatus* and *Rhodopseudomonas viridis*. *Biochemistry* **32**, 4793-4800
26. Wagner, G., Hyberts, S.G., and Havel, T.F. (1992) NMR structure determination in solution: A critique and comparison with X-ray crystallography. *Annu. Rev. Biophys. Biomol. Struct.* **21**, 167-198
27. Donohue, T.J., McEwan, A.G., and Kaplan, S. (1986) Cloning, sequence and expression of the *Rhodobacter sphaeroides* cytochrome c_2 gene. *J. Bacteriol.* **168**, 962-972

Downloaded from http://jb.oxfordjournals.org/ at Changhua Christian Hospital on October 2, 2012

28. Brandner, J.P., McEwan, A.G., Kaplan, S., and Donohue, T.J. (1989) Expression of the *Rhodobacter sphaeroides* cytochrome c_2 structural gene. *J. Bacteriol.* **171**, 360-368
29. Meyer, T.E. and Cusanovich, M.A. (1985) Soluble cytochrome composition of the purple phototrophic bacterium, *Rhodopseudomonas sphaeroides* ATCC 17023. *Biochim. Biophys. Acta* **807**, 308-319
30. Rance, M., Sørensen, O.W., Bodenhausen, G., Wagner, G., Ernst, R.R., and Wüthrich, K. (1983) Improved spectral resolution in COSY ^{1}H NMR spectra of proteins via double quantum filtering. *Biochem. Biophys. Res. Commun.* **117**, 479-485
31. Braunschweiler, L. and Ernst, R.R. (1983) Coherence transfer by isotopic mixing: Application to proton correlation spectroscopy. *J. Magn. Reson.* **53**, 521-528
32. Davis, D.G. and Bax, A. (1985) Assignment of complex ^{1}H NMR spectra via two-dimensional homonuclear Hartmann-Hahn spectroscopy. *J. Am. Chem. Soc.* **107**, 2820-2821
33. Jeener, J., Meier, B.H., Bachmann, P., and Ernst, R.R. (1979) Investigation of exchange processes by two-dimensional NMR spectroscopy. *J. Chem. Phys.* **71**, 4546-4553
34. Macura, S., Hyang, Y., Suter, D., and Ernst, R.R. (1981) Two-dimensional chemical exchange and cross-relaxation spectroscopy of coupled nuclear spins. *J. Magn. Reson.* **43**, 259-281
35. States, D.J., Haberkorn, R.A., and Ruben, D.J. (1982) A two-dimensional nuclear overhauser experiment with pure absorption phase in four quadrants. *J. Magn. Reson.* **48**, 286-292
36. Plateau, P. and Guéron, M. (1982) Exchangeable proton NMR without base-line distortion, using new strong-pulse sequences. *J. Am. Chem. Soc.* **104**, 7310-7311
37. Griesinger, C., Otting, G., Wüthrich, K., and Ernst, R.R. (1988) Clean TOCSY for ^{1}H spin system identification in macromolecules. *J. Am. Chem. Soc.* **110**, 7870-7872
38. Freeman, R., Friedrich, J., and Wu, X.-L. (1988) A pulse for all seasons. Fourier transform spectra without a phase gradient. *J. Magn. Reson.* **79**, 561-567
39. Bodenhausen, G. and Ruben, D. (1980) Natural abundance nitrogen-15 NMR by enhanced heteronuclear spectroscopy. *Chem. Phys. Lett.* **69**, 185-189
40. Bax, A. and Pochapsky, S. (1992) Optimized recording of heteronuclear multidimensional NMR spectra using pulsed field gradients. *J. Magn. Reson.* **99**, 638-643
41. Messerle, B.A., Wider G., Otting G., Weber C., and Wüthrich, K. (1989) Solvent suppression using a spin lock in 2D and 3D NMR spectroscopy with H_2O solutions. *J. Magn. Reson.* **85**, 608-613
42. Tate, S.-I., Masui, Y., and Inagaki, F. (1991) Spin-lock pulses for purging and shaping the water resonance in ^{1}H-detected ^{15}N single-quantum-coherence spectroscopy. *J. Magn. Reson.* **94**, 394-400
43. Marion, D., Ikura, M., Tschudin, R., and Bax, A. (1989) Rapid recording of 2D NMR spectra without phase cycling. Application to the study of hydrogen exchange in proteins. *J. Magn. Reson.* **85**, 393-399
44. Sklenár, V., Piotto, M., Leppik., and Saudek, V. (1993) Gradient-tailored water suppression for ^{1}H-^{15}N HSQC experiments optimized to retain full sensitivity. *J. Magn. Reson.* **102**, 241-245
45. Medvedeva, S., Simorre, J.-P., Brutscher, B., Guerlesquin, F., and Marion, D. (1993) Extensive ^{1}H NMR resonance assignment of proteins using natural abundance gradient-enhanced ^{13}C-^{1}H correlation spectroscopy. *FEBS Lett.* **333**, 251-256
46. Vuister, G. and Bax, A. (1993) Quantitative J correlation: A new approach for measuring homonuclear three-bond J(H^{N}H$^\alpha$) coupling constants in ^{15}N-enriched proteins. *J. Am. Chem. Soc.* **115**, 7772-7777
47. Kay, L., Marion, D., and Bax, A. (1989) Practical aspects of 3D heteronuclear NMR of proteins. *J. Magn. Reson.* **84**, 72-84
48. Marion, D., Driscoll, P., Kay, L., Wingfield, P., Bax, A., Gronenborn, A., and Clore, G. (1989) Overcoming the overlap problem in the assignment of ^{1}H NMR spectra of larger proteins by use of three-dimensional heteronuclear ^{1}H-^{15}N Hartmann-Hahn-multiple quantum coherence and nuclear Overhauser-multiple quantum coherence spectroscopy: Application to interleukin 1β. *Biochemistry* **28**, 6150-6156
49. Caffrey, M., Brutscher, B., Simorre, J.-P., Fitch, J., Cusanovich, M., and Marion, D. (1994) Assignment of the ^{13}C and ^{13}CO resonances for *Rhodobacter capsulatus* ferrocytochrome c_2 using double-resonance and triple-resonance NMR spectroscopy. *Eur. J. Biochem.* **221**, 63-75
50. Petillot, Y., Forest, E., Mathieu, I., Meyer, J., and Moulis, J.-M. (1993) Analysis by electrospray ionization mass spectrometry of several forms of *Clostridium pasteurianum* rubredoxin. *Biochem. J.* **296**, 657-661
51. Ambler, R.P., Daniel, M., Hermoso, J., Meyer, T.E., Bartsch, R.G., and Kamen, M.D. (1979) Cytochrome c_2 sequence variation among recognised species of purple non-sulfur photosynthetic bacteria. *Nature* **278**, 661-662
52. Gooley, P., Caffrey, M., Cusanovich, M., and MacKenzie, N. (1990) Assignment of the ^{1}H and ^{15}N spectra of *Rhodobacter capsulatus* ferrocytochrome c_2. *Biochemistry* **29**, 2278-2290
53. Wand, A.J., Di Stefano, D.L., Feng, Y., Roder, H., and Englander, S.W. (1989) Proton resonance assignments of horse ferrocytochrome *c*. *Biochemistry* **28**, 186-194
54. Keller, R.M. and Wüthrich, K. (1978) Evolutionary change of the heme *c* structure: Ferricytochrome *c*-551 from *Pseudomonas aeruginosa* and horse heart ferricytochrome *c*. *Biochem. Biophys. Res. Commun.* **83**, 1132-1139
55. Wüthrich, K. (1986) *NMR of Proteins and Nucleic Acids*, John Wiley & Sons, New York
56. Moore, G. and Pettigrew, G. (1990) *Cytochromes c: Evolutionary, Structural and Physiological Aspects*, Springer-Verlag, Berlin
57. Morelle, N., Simorre, J.-P., Caffrey, M., Meyer, T., Cusanovich, M., and Marion, D. (1995) ^{1}H and ^{13}C NMR assignment and secondary structure of *Chlorobium limicola f. thiosulfatophilum* ferrocytochrome c_{555}. *FEBS Lett.* **365**, 172-178
58. Benning, M., Meyer, T., and Holden, H. (1994) X-ray structure of the cytochrome c_2 isolated from *Paracoccus denitrificans* refined at 1.7-Å resolution. *Arch. Biochem. Biophys.* **310**, 460-466
59. Pettigrew, G. and Moore, G. (1987) *Cytochromes c: Biological Aspects*, Springer-Verlag, Berlin

Downloaded from http://jb.oxfordjournals.org/ at Changhua Christian Hospital on October 2, 2012